Engineering 2015, 1(3): 336–343
DOI 10.15302/J-ENG-2015079

Research
Medical Instrumentation—Article

An Ultrasonic Backscatter Instrument for Cancellous Bone Evaluation in Neonates

Chengcheng Liu[1], Rong Zhang[2], Ying Li[1], Feng Xu[1], Dean Ta[1,3]*, Weiqi Wang[1]

ABSTRACT Ultrasonic backscatter technique has shown promise as a noninvasive cancellous bone assessment tool. A novel ultrasonic backscatter bone diagnostic (UBBD) instrument and an *in vivo* application for neonatal bone evaluation are introduced in this study. The UBBD provides several advantages, including noninvasiveness, non-ionizing radiation, portability, and simplicity. In this study, the backscatter signal could be measured within 5 s using the UBBD. Ultrasonic backscatter measurements were performed on 467 neonates (268 males and 199 females) at the left calcaneus. The backscatter signal was measured at a central frequency of 3.5 MHz. The delay (T_1) and duration (T_2) of the backscatter signal of interest (SOI) were varied, and the apparent integrated backscatter (AIB), frequency slope of apparent backscatter (FSAB), zero frequency intercept of apparent backscatter (FIAB), and spectral centroid shift (SCS) were calculated. The results showed that the SOI selection had a direct influence on cancellous bone evaluation. The AIB and FIAB were positively correlated with the gestational age ($|R|$ up to 0.45, $P < 0.001$) when T_1 was short (< 8 μs), while negative correlations ($|R|$ up to 0.56, $P < 0.001$) were commonly observed for $T_1 > 10$ μs. Moderate positive correlations ($|R|$ up to 0.45, $P < 0.001$) were observed for FSAB and SCS with gestational age when T_1 was long (> 10 μs). The T_2 mainly introduced fluctuations in the observed correlation coefficients. The moderate correlations observed with UBBD demonstrate the feasibility of using the backscatter signal to evaluate neonatal bone status. This study also proposes an explicit standard for *in vivo* SOI selection and neonatal cancellous bone assessment.

KEYWORDS ultrasonic backscatter, cancellous bone evaluation, signal of interest (SOI), backscatter instrument, neonatal bone status

1 Introduction

Currently, bone-status assessment is mainly based on X-ray densitometry techniques such as quantitative computed tomography (QCT), dual-energy X-ray absorptiometry (DXA), and peripheral quantitative computed tomography (pQCT) [1, 2]. The bone mineral density (BMD) provided by DXA is widely used in clinics to evaluate bone quality and predict the risk of bone fracture [3–5]. However, one disadvantage of these X-ray-based methods is the ionizing radiation that restricts their application in specialized populations such as pregnant women and newborn babies. Therefore, developing an alternative technique is of great significance. Quantitative ultrasound (QUS) has drawn great attention as a noninvasive tool for bone-status evaluation [6–11]. Besides the advantages in safety, non-ionizing radiation, portability, and low cost, the ultrasound can reflect information about the bone structure and elastic modulus. QUS for cancellous bone evaluation is mainly classified into two methods: through-transmission and backscattering. Through-transmission measurements use two transducers, one as the transmitter and one as the receiver. These types of measurements are typically performed on skeletal sites that are accessible by two transducers, such as the calcaneus. The broadband ultrasound attenuation (BUA) and speed of sound (SOS) are the two most common through-transmission parameters [12–14]. Numerous clinical QUS instruments have been developed based on the through-transmission method [7, 15–17]. Over the last few decades, researchers have focused on the ultrasonic backscatter technique for cancellous bone evaluation [9–11, 18]. Unlike through-transmission measurements, the backscatter technique uses a single transducer to both transmit and receive ultrasonic signals and can provide easier access to osteoporosis-sensitive bones, such as the hip and spine. Several studies have demonstrated that the backscatter signal is closely related to bone characteristics including number density, BMD, ultimate strength, size, shape, and elastic properties [19–28]. The backscatter signal is sensitive to the microstructure of cancellous bone, making it feasible to extract trabecular microstructural information from the backscatter signal [29, 30]. Recently, some studies performed *in vivo* backscatter

[1] Department of Electronic Engineering, Fudan University, Shanghai 200433, China; [2] Department of Neonatology, Children's Hospital of Fudan University, Shanghai 201102, China; [3] Key Laboratory of Medical Imaging Computing and Computer Assisted Intervention (MICCAI) of Shanghai, Shanghai 200032, China
* Correspondence author. E-mail: tda@fudan.edu.cn
Received 3 August 2015; received in revised form 27 August 2015; accepted 4 September 2015

measurements and investigated the feasibility of using the backscatter signal to evaluate bone status in the clinic [11, 28, 31–34]. In a previous study, we investigated the influence of the selected backscatter signal on measured values of the backscatter parameters and proposed a signal-selection standard for the backscatter measurement of cancellous bone *in vitro* [35]. The *in vivo* signal-selection standard for cancellous bone evaluation is waiting to be analyzed.

The bone nutritional status in neonates and early childhood stages is significantly related to skeletal development later in life [32, 36]. Lacking the ability to store calcium and phosphorus at birth, neonates have a high risk for metabolic bone disease [37–39]. Therefore, it is of great interest to monitor bone nutritional status in order to prevent metabolic bone diseases in neonates. Currently, neonatal bone evaluation is based on a blood test for specific biochemical markers. However, the biochemical markers (serum calcium, phosphorous, and alkaline phosphatase) are only weakly correlated with BMD [40, 41]. Furthermore, blood tests are invasive and not usually preferred for neonates, especially preterm infants. X-ray-based densitometry techniques are not typically used in newborn infants because of the ionizing radiation and relatively low sensitivity [42]. Compared with the routine X-rays and biochemical markers, QUS is safer and can easily be performed on neonates. Previously, researchers have investigated the feasibility of QUS for neonatal bone assessment [32, 39].

We developed a novel ultrasonic backscatter bone diagnostic (UBBD) instrument based on the ultrasonic backscatter method. The UBBD provides several advantages, including noninvasiveness, non-ionizing radiation, portability, and simplicity. Recently, the UBBD was used to perform backscatter measurements on adults and newborn babies. Jiang et al. demonstrated that the calcaneus backscatter signal measured with the UBBD was significantly correlated with the BMD in hip and spine (R = 0.63–0.75, P < 0.05) [31]. Zhang et al. measured the backscatter signal in neonates with the UBBD, and found a significant correlation between the backscatter coefficient (BSC) and gestational age and birth length (R = 0.43–0.47, P < 0.001) [32]. These studies demonstrate the utility of the UBBD in the backscatter measurement of cancellous bone *in vivo*.

In this study, we performed backscatter measurements on 467 neonates (268 males and 199 females) at the left calcaneus using the UBBD and investigated the feasibility of using the backscatter signal to characterize neonatal bone status. The influence of the selected backscatter signal of interest (SOI) on the neonatal bone assessment was analyzed. This study also optimized the SOI selection and attempted to propose an explicit standard for *in vivo* SOI selection in neonatal cancellous bone assessment.

2 Material and methods

2.1 UBBD instrument

The UBBD was developed based on a Linux-embedded system and has two modules: the ultrasonic signal transmit and receive (USTR) module, and the data-processing and display (DPD) module, as shown in Figure 1(a). The USTR module was based on the field-programmable gate array (FPGA). In the USTR module, a short pulse with a voltage of approximately ± 50 V was produced to excite the ultrasonic transducer. The backscatter signal received by the same transducer underwent pre-processing and amplification, and was passed through gain-compensation circuits, followed by high-speed analog to digital conversion. Next, the digital backscatter signal was concurrently transmitted to the DPD module. An ARM9 processer was used as the central processing unit in the DPD module. The backscatter signal was analyzed and the backscatter parameters were calculated in the DPD module. Results were displayed on a liquid crystal display (LCD) with a touch screen (9 in, 1 in = 2.54 cm). An external keyboard/mouse and mini-printer were also employed in this instrument.

An interactive interface was developed for the UBBD (Figure 1(b)). Transducers with different central frequencies were interchangeable. The system emitted a short (2 μs) single-cycle sinusoidal pulse for pulse-echo tissue insonification. The echoes were received by the same transducer, amplified and digitized with 12-bit accuracy at data rates as high as 40 000 000 samples per second. The backscatter signal was obtainable within 5 s. To reduce random noise, 128 waveforms were averaged in the time domain and then stored in the system for analysis.

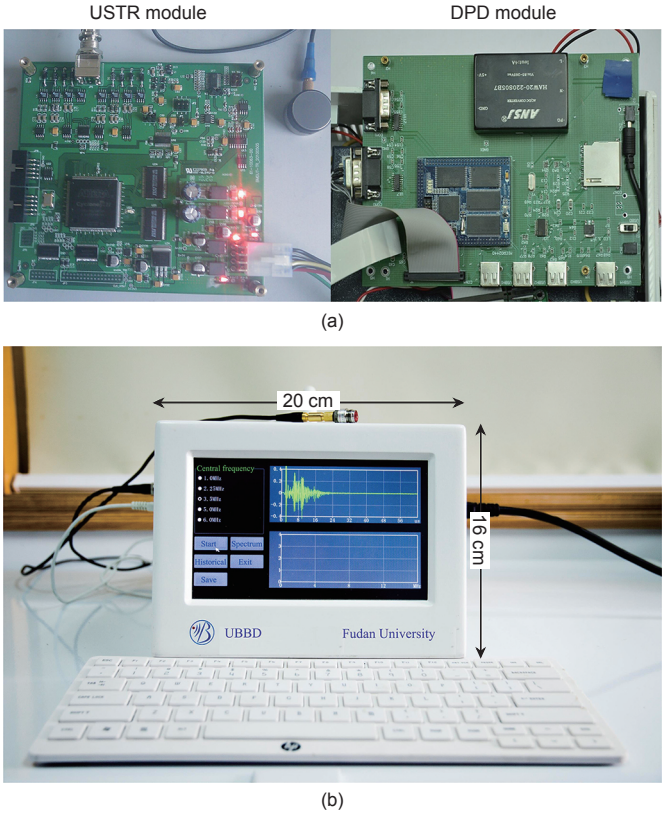

Figure 1. (a) The inner functional modules; (b) the surface appearance of the UBBD.

2.2 Subjects and anthropometry

A total of 467 neonates (268 males and 199 females) hospitalized in the Neonatal Department in the Children's Hospital of Fudan University, Shanghai, China, participated in this

study. The following exclusion criteria were adopted: congenital malformation, inherited metabolic diseases, abnormalities of the digestive system, or bone diseases. Gestational age was recorded, along with the length, weight, and head circumference at the time of birth. Table 1 lists the anthropometric characteristics of the participated subjects.

Table 1. Anthropometric characteristics of the subjects.

	Male	Female
Number	268	199
Gestational age (days)	253.9 ± 23.3	253.8 ± 25.7
Birth weight (g)	2709.2 ± 824.9	2566.9 ± 839.9
Birth length (cm)	32.4 ± 2.4	31.9 ± 2.6
Head circumference (cm)	47.1 ± 4.2	46.3 ± 4.7

Note: Values are mean ± standard deviation (SD).

This study was approved and conducted by the ethics committee of the Children's Hospital of Fudan University, and informed consent was obtained from all parents.

2.3 Backscatter measurements

Backscatter measurements were performed with the UBBD. An unfocused transducer with a central frequency of 3.5 MHz (V546, Olympus-Panametrics Inc., Waltham, MA, USA) was used. The diameter of the transducer was 0.25 in and the –6 dB bandwidth was 3.07 MHz (1.62–4.69 MHz). As shown in Figure 2(a), the transducer was placed vertically on the inner part of the heel and the backscatter signal was measured at the left calcaneus for each subject. Ultrasonic gel (Echo Jelly; Aloka Medical Equipment Co., Shanghai, China) was used to couple the transducer to the soft tissue atop the calcaneus of the subject. The sampling frequency of the UBBD was set to 32.0 MHz. A typical backscattered signal acquired from a neonatal calcaneus at 3.5 MHz is shown in Figure 2(b). The signal reflected by a polished steel plate placed in pure water was obtained as the reference signal (shown in Figure 2(c)). After recording calcaneus backscatter signals in neonates, the UBBD system processed and analyzed the data.

2.4 Signal analysis

The signals shown in Figure 2(b) consist of the excited signal (duration: 0–2 μs), the signals reflected by the soft tissue and the cortical bone (approximately 6–10 μs), and the backscatter signal from the trabecular bone (10–20 μs). Analysis of the backscattered signal of interest required excluding the signals reflected and backscattered by the soft tissue and cortical bone. As illustrated in Figure 2(b), a rectangular window was used to select the backscatter SOI. The time window was positioned with a time delay after 6 μs. The delayed amount was defined as T_1 and the length of the time window was defined as T_2. The backscatter parameters were calculated with the selected SOI.

The apparent backscatter coefficient (ABC(f)) is a function of the frequency and was defined as follows [23, 24]:

$$\mathrm{ABC}(f) = 20\lg\frac{S_{\mathrm{SOI}}(f)}{S_{\mathrm{R}}(f)} \tag{1}$$

where $S_{\mathrm{SOI}}(f)$ and $S_{\mathrm{R}}(f)$ are the amplitude spectrum of the backscattered SOI and the reference signal, respectively.

The apparent integrated backscatter (AIB) is the averaged or integrated value of ABC in the effective frequency band $[f_{\min}, f_{\max}]$:

$$\mathrm{AIB} = \frac{\int_{f_{\min}}^{f_{\max}} \mathrm{ABC}(f)\mathrm{d}f}{f_{\max} - f_{\min}} \tag{2}$$

Linear regression was performed on the ABC(f) in the frequency band of interest. The frequency slope of apparent backscatter (FSAB) and zero frequency intercept of apparent backscatter (FIAB) were determined as the slope and the zero frequency intercept of the line fitted to the ABC(f), respectively [20].

The spectral centroid shift (SCS) was defined as follows [28, 31]:

$$\mathrm{SCS} = \frac{\int_{f_{\min}}^{f_{\max}} f \cdot S_{\mathrm{SOI}}(f)\mathrm{d}f}{\int_{f_{\min}}^{f_{\max}} S_{\mathrm{SOI}}(f)\mathrm{d}f} - f_0 \tag{3}$$

where $S_{\mathrm{SOI}}(f)$ is the amplitude spectrum of the backscattered SOI; $[f_{\min}, f_{\max}]$ corresponds to the –6 dB frequency band of the transducer; and f_0 is the central frequency of the transducer. The effective frequency band was 1.62–4.69 MHz in this analysis.

Manipulation of the delay (T_1) and duration (T_2) of the time window allowed for the calculation of AIB, FSAB, FIAB, and SCS with different SOIs.

2.5 Statistical analysis

The mean and standard deviation (SD) values of the anthropometric parameters of the subjects were calculated (Table 1). The relationship between the four backscatter parameters

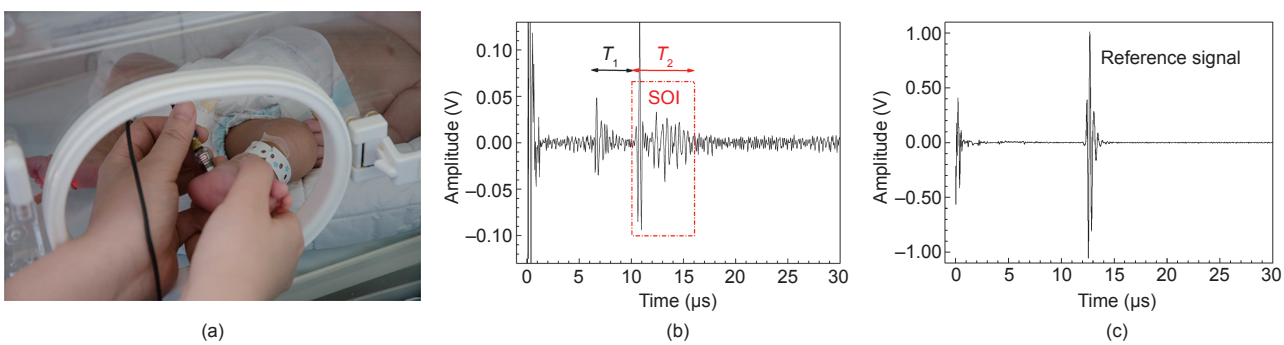

Figure 2. (a) Backscatter measurement performed at neonatal calcaneus; (b) the measured backscatter signal; (c) the reference signal.

under different SOI selections and each of the four anthropometric parameters was examined using scatter plots. Linear regression analysis was performed to determine the correlation of the backscatter parameters with the anthropometric parameters. Statistical significance was tested using one-way analysis of variance (ANOVA). A $P < 0.01$ was considered to be statistically significant.

3 Results

The backscatter SOI was varied through changes in T_1 and T_2. The correlation between the corresponding backscatter parameters (AIB, FIAB, FSAB, and SCS) and each of the neonatal anthropometric parameters was calculated. The relationship among the neonatal anthropometric parameters was also analyzed. The influence of the SOI selection on the backscatter parameters for neonatal bone evaluation was determined.

3.1 The relationship among the four anthropometric parameters

Table 2 shows the correlation among the anthropometric parameters. Significantly strong correlations (R = 0.81–0.92, $P < 0.001$) were observed between the gestational age, birth weight, head circumference, and birth length. The anthropometric parameters were used to characterize the neonatal nutritional status and reflected the bone nutritional status as well. Since the four anthropometric parameters were highly correlated with each other, the gestational age was used as the representative anthropometric for the following analysis.

3.2 The influence of SOI selection on AIB for neonatal bone evaluation

Figure 3 shows the relationship between AIB and gestational age under two typical SOI selections. The AIB was found to be positively correlated with the gestational age (R = 0.45, $P < 0.001$) for T_1 = 6.50 μs and T_2 = 2.34 μs. A negative correlation (R = –0.56, $P < 0.001$) was observed between AIB and gestational age with T_1 = 12.75 μs and T_2 = 7.03 μs. The influence of SOI selection on the observed correlation coefficient (red for 1 and blue for –1) for AIB versus gestational age and AIB versus birth weight are shown in Figure 4(a) and Figure 4(b), respectively. In general, positive correlations ($|R|$ up to 0.45, $P < 0.001$) were observed when T_1 was short (< 8 μs), while negative correlations ($|R|$ up to 0.56, $P < 0.001$) were more common for T_1 greater than 10 μs. The phenomena for AIB versus birth weight were quite similar to the correlations between AIB and gestational age, with AIB versus birth weight showing moderate correlation ($|R|$ up to 0.55, $P < 0.001$).

Table 2. Correlations between the anthropometric parameters of the neonates.

Variables	Correlation coefficient			
	Gestational age	Birth weight	Head circumference	Birth length
Gestational age	1	—	—	—
Birth weight	0.84**	1	—	—
Head circumference	0.81**	0.87**	1	—
Birth length	0.84**	0.92**	0.91**	1

Note: **: $P < 0.001$.

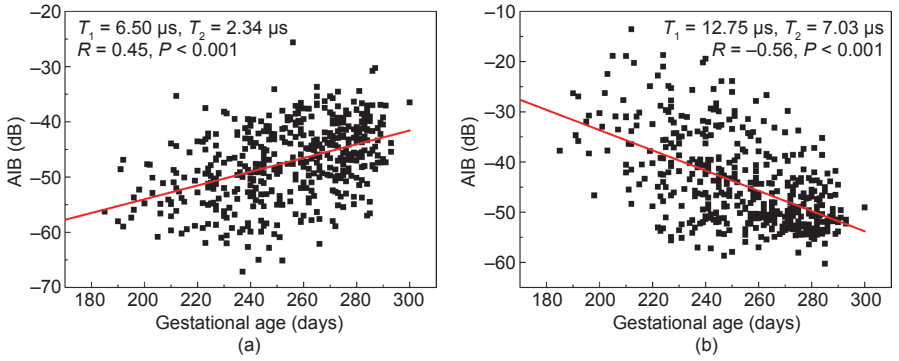

Figure 3. The relationship between AIB and gestational age for two typical SOIs. (a) T_1 = 6.50 μs, T_2 = 2.34 μs; (b) T_1 = 12.75 μs, T_2 = 7.03 μs.

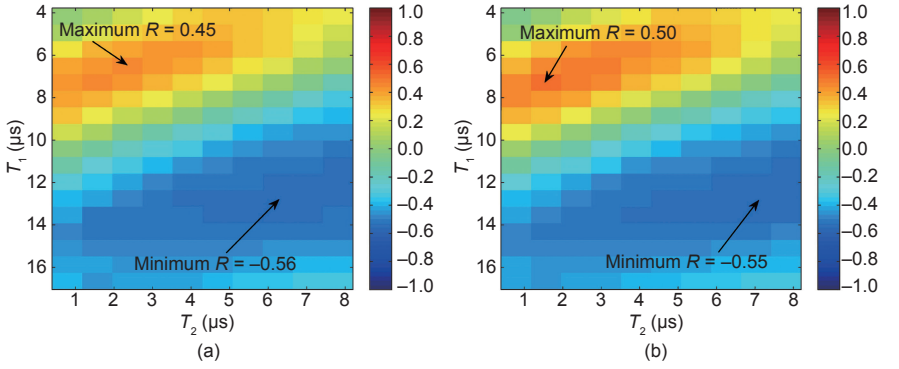

Figure 4. The effect of SOI selection on the correlations between AIB and (a) gestational age, (b) birth weight.

3.3 The influence of SOI selection on FIAB and FSAB for neonatal bone evaluation

The correlation coefficients for FIAB and gestational age plotted as a function of the T_1 and T_2 are shown in Figure 5(a) and Figure 5(b), respectively. In Figure 5(a), the correlation was positive when T_1 was below 8 μs. The correlation coefficient decreased and eventually turned to negative with increasing T_1. Negative correlations (R = –0.50, $P < 0.001$) were observed when T_1 was approximately 13 μs. In Figure 5(b), the correlation coefficient tended to decrease as T_2 increased such that the positive correlations weakened while the negative correlations strengthened with increasing T_2.

3.4 The influence of SOI selection on FSAB for neonatal bone evaluation

Figure 6 shows the correlation coefficients between FSAB and gestational age. Gen-

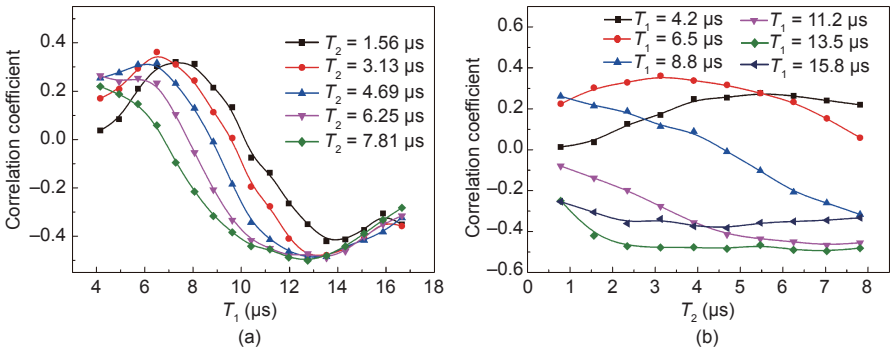

Figure 5. The correlation coefficient between FIAB and gestational age plotted as a function of (a) T_1 and (b) T_2.

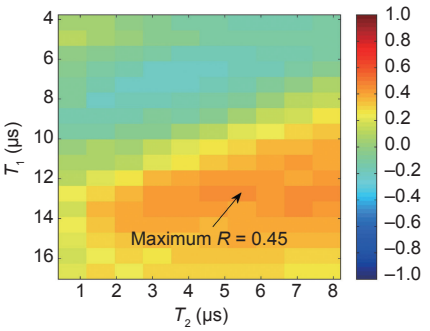

Figure 6. The effect of SOI selection on the correlations between FSAB and gestational age.

erally speaking, significantly positive correlations were observed when T_1 was longer than 10 μs. The correlation coefficient was 0.45 when T_1 was 12.75 μs and T_2 was 5.45 μs. However, when the T_1 was short (< 10 μs), the correlations were quite weak and insignificant. T_2 had little effect on the correlations, and the correlations did not change when T_2 was relatively long (> 3 μs).

3.5 The influence of SOI selection on SCS for neonatal bone evaluation

Figure 7(a) shows the correlation coefficient for SCS and gestational age plotted as a function of T_1 with respect to some T_2 values. The correlations were quite weak and insignificant when T_1 was short (< 10 μs). With increasing T_1, the correlations turned negative and increased. Moderate correlations (R = 0.41, P < 0.001) were observed when T_1 was around 13 μs. Figure 7(b) plots the correlation coefficient for SCS and gestational age as a function of T_2. T_2 has a complex effect on the observed correlations, which means that as the analyzed SOI length varied, the backscatter spectrum also varied.

4 Discussion

It is well known that bone development is significantly correlated with gestational age, birth weight, and birth length [43–45]. These anthropometric characteristics reflect the skeletal development of neonates and can be used as an index of neonatal bone status. This study analyzed the relationship between the backscatter signal and gestational age, birth weight, birth length, and head circumference. The results showed that the backscatter signal could be significantly correlated with the anthropometric characteristics of the neonates.

Studies have indicated that the microstructure of cancellous bone reflects the bone nutritional status in neonates. Neonates with metabolic bone diseases have significant abnormalities in the microstructure of cancellous bone [45]. Therefore, measuring cancellous bone could help assess bone nutritional status in neonates. The calcaneus was chosen as the site of interest in this study as the bone tissue in the calcaneus is mainly cancellous bone and is easily accessible. The outer cortical shell and the overlying soft tissue in the calcaneus are relatively thin and flat, making it straightforward to place the transducer.

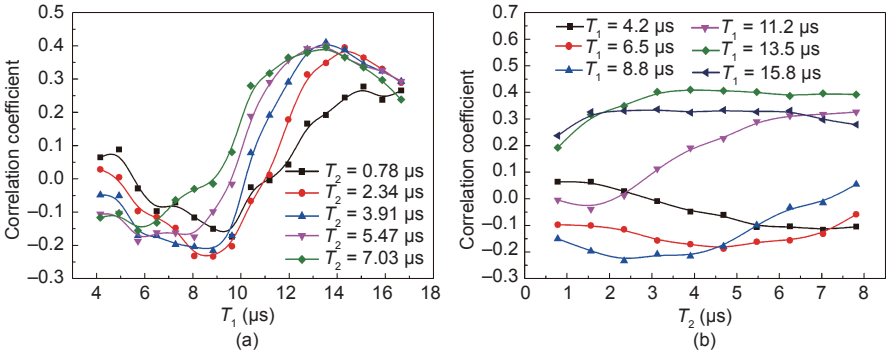

Figure 7. The correlation coefficient between SCS and gestational age plotted as a function of (a) T_1 and (b) T_2.

The apparent backscatter was not compensated for the frequency-dependent diffraction and attenuation effects. Therefore, in addition to the backscatter effect, the apparent backscatter parameters (AIB, FSAB, and FIAB) were sensitive to attenuation. The correlation between the apparent backscatter parameters and gestational age resulted from the combined effects of backscatter and attenuation. The correlation (negative or positive) depended primarily on which effect was dominant. When T_1 was short (i.e., ultrasonic propagation length was small), the attenuation effect was lower than the backscatter effect and the backscatter effect dominated the observed correlation. For neonates with longer gestational age, the dominance of the backscatter effect was more pronounced than that of the attenuation effect, so the AIB and FIAB values were larger. Therefore, positive correlations were observed for AIB and FIAB with gestational age when T_1 was short. In contrast, when T_1 was sufficiently long, the attenuation effect (increasing exponentially with the ultrasonic propagation length) dominated the observed correlation. Neonates with longer gestational age had smaller AIB and FIAB values and larger FSAB. This observation is the reason for negative correlations for AIB and FIAB with gestational age and positive correlation for FSAB with gestational age when T_1 was long. However, it was found that T_1 should not be > 16 μs because of heavy

attenuation yielding a small SOI with a poor signal-to-noise ratio, which may influence the accuracy of the cancellous bone assessment. The T_2 was the SOI length, corresponding to the ultrasonically interrogated trabecular volume. Because cancellous bone is anisotropic and inhomogeneous, the backscatter cross-section varied and the backscatter signal fluctuated as T_2 changed. Therefore, the correlations for the backscatter parameters with gestational age fluctuated as T_2 varied. Our recent work analyzed the influence of the SOI on the apparent backscatter measurement of cancellous bone *in vitro* [35]. Significantly positive correlations between AIB and bone volume fraction (bone volume/total volume, BV/TV) were observed for short T_1 and negative correlations were observed when T_1 was long for the frequency range 0.5–10 MHz. These *in vitro* results are consistent with the present *in vivo* findings.

Ultrasonic waves are attenuated as a function of frequency during propagation through biological tissues. In general, the frequency-dependent attenuation has an effect similar to that of a low-pass filter: The signals at higher frequencies are attenuated more than the signals at lower frequencies. As a result, the centroid of the backscattered spectrum is downshifted to a lower value compared with the original spectrum. When a Gaussian pulse propagates in a medium with linear frequency dependence of attenuation, the Gaussian spectrum retains its Gaussian form while the SCS is proportional to the product of the attenuation coefficient, the propagating distance, and the square of the bandwidth [46]. The propagating distance corresponded to T_1 in this study. As T_1 increased, the SCS was more pronounced. This may explain why significant correlations were observed for SCS and gestational age only when T_1 was sufficiently long (approximately 12–16 μs). Note that the backscattered SCS is affected by all of the frequency-dependent factors: attenuation in soft tissue, cortical bone and trabecular bone, transmission coefficients of cortical bone, and multiple scattering effects.

The present study found that the apparent backscatter was significantly correlated with gestational age ($|R|$ up to 0.45, $P < 0.001$) for short T_1 (< 8 μs), and negative correlations ($|R|$ up to 0.56, $P < 0.001$) for long T_1 (> 10 μs). These findings are consistent with our previous study, which found the ABC to be positively correlated with gestational age (R = 0.19–0.47) for T_1 < 2 μs and T_2 = 8 μs [32]. Zhang et al. also found that gender had no influence on bone status at birth [32]. Skeletal development differences between male and female adults are more closely associated with hormone levels, exercise status, and other physiological and environmental factors [43, 44]. Therefore, this study did not analyze data based on gender. We did not consider phase interference in the analysis of the backscatter parameters. Phase interference usually occurs in ultrasonic backscatter signals. The constructive or destructive interferences of ultrasonic waves might introduce random errors in the measured backscatter parameters. Phase interference might be one explanation of the weak correlations observed in this study. Due to heavy attenuations in cancellous bone, transducers with lower frequencies (1 MHz or 2.25 MHz) are preferred for cancellous bone assessment for the adult. Considering that the neonatal calcaneus is quite tiny and cancellous bone is not well-developed, transducers with relatively higher frequencies (3.5 MHz and 5 MHz) are usually recommended [32]. Therefore, we used a transducer with a central frequency of 3.5 MHz in this study. We only measured the backscatter signal at the calcaneus for each neonate and did not perform the spatial scanning and average. The highly statistical variance of the cancellous bone structure might have introduced some random errors. If spatial averaging was P performed, the observed correlations between backscatter parameters and anthropometric characteristics of neonates might be stronger.

Other authors have performed ultrasonic transmission measurements in neonates and found that QUS parameters were closely correlated with gestational age and birth weight [39, 43–45]. Teitelbaum et al. obtained a positive correlation between SOS in cortical bone and birth weight (R = 0.3; P < 0.001) [39]. Rack et al. found that QUS values from the first week of life were significantly correlated with gestational age (R = 0.5, P < 0.001), and follow-up measurements correlated positively with weight during the week of measurement (R = 0.4; P = 0.001) [47]. These studies demonstrate that QUS transmission parameters could be used to evaluate bone status in neonates. The present study performed backscatter measurements and demonstrated that the apparent backscatter could be more conveniently used to evaluate neonatal bone status with moderate correlations. This study also analyzed the SOI influence on apparent backscatter measurements of cancellous bone in neonates. Table 3 summarizes the optimization of the observed correlations with explicit SOI selections. The results can provide constructive suggestions for *in vivo* SOI selection in neonatal cancellous bone assessment.

Table 3. Optimization of the observed correlations with explicit SOI selections.

Ultrasonic parameter	Neonatal parameter	Frequency (MHz)	T_1 (μs)	T_2 (μs)	Correlation coefficient	Correlations
AIB	Gestational age	3.5	6.50	2.34	0.45	Positive
			12.75	7.03	–0.56	Negative
FIAB	Gestational age	3.5	6.50	3.13	0.36	Positive
			12.75	7.03	–0.50	Negative
FSAB	Gestational age	3.5	12.75	5.47	0.45	Positive
SCS	Gestational age	3.5	13.53	3.91	0.41	Positive

This study introduced the UBBD, an ultrasonic backscatter instrument for cancellous bone evaluation. Other studies have also used the UBBD for the backscatter measurements. Jiang et al. measured the backscatter signal at the adult calcaneus with UBBD and found that backscatter signal was correlated with hip and spine BMD (R = 0.63–0.75, P < 0.05) [31]. Zhang et al. also performed backscatter measurement in neonatal calcaneus with UBBD and demonstrated that the BSC could be used to assess bone nutritional status in neonates [32]. These studies demonstrate the utility of the UBBD in backscatter measurement of cancellous bone *in vivo*.

5 Summary

The present study performed *in vivo* backscatter measure-

ments of the calcaneus in neonates with the self-developed UBBD. Through changes in SOI selection, the backscatter parameters were calculated and the influence of SOI selection on the apparent backscatter measurement of neonatal cancellous bone was investigated. We found that the SOI selection significantly affected the correlations between the backscatter and the anthropometric characteristics of neonates. The AIB and FIAB were positively correlated with gestational age (R^2 up to 0.20, $P < 0.001$) for short T_1 (< 8 μs), while negative correlations (R^2 up to 0.31, $P < 0.001$) were commonly observed for $T_1 > 10$ μs. Moderate positive correlations (R^2 up to 0.20, $P < 0.001$) were observed for FSAB and SCS with gestational age when T_1 was long (> 10 μs). Based on the results, this study proposed an explicit standard for *in vivo* SOI selection and neonatal cancellous bone assessment.

Acknowledgements

This work was supported by the National Natural Science Foundation of China (11174060, 11327405, and 11504057), the Science and Technology Support Program of Shanghai (13441901900), the PhD Programs Foundation of the Ministry of Education of China (20130071110020), and the China Postdoctoral Science Foundation (2015M571490).

Compliance with ethics guidelines

Chengcheng Liu, Rong Zhang, Ying Li, Feng Xu, Dean Ta, and Weiqi Wang declare that they have no conflict of interest or financial conflicts to disclose.

References

1. K. Engelke, et al. Clinical use of quantitative computed tomography and peripheral quantitative computed tomography in the management of osteoporosis in adults: The 2007 ISCD Official Positions. *J. Clin. Densitom.*, 2008, 11(1): 123–162
2. R. Lorente-Ramos, J. Azpeitia-Armán, A. Muñoz-Hernández, J. M. García-Gómez, P. Díez-Martínez, M. Grande-Bárez. Dual-energy X-ray absorptiometry in the diagnosis of osteoporosis: A practical guide. *AJR Am. J. Roentgenol.*, 2011, 196(4): 897–904
3. P. Andreopoulou, R. S. Bockman. Management of postmenopausal osteoporosis. *Annu. Rev. Med.*, 2015, 66: 329–342
4. C. B. Becker. Sclerostin inhibition for osteoporosis—A new approach. *N. Engl. J. Med.*, 2014, 370(5): 476–477
5. T. D. Rachner, S. Khosla, L. C. Hofbauer. Osteoporosis: Now and the future. *Lancet*, 2011, 377(9773): 1276–1287
6. P. Laugier. Quantitative ultrasound of bone: Looking ahead. *Joint Bone Spine*, 2006, 73(2): 125–128
7. D. Mulleman, I. Legroux-Gerot, B. Duquesnoy, X. Marchandise, B. Delcambre, B. Cortet. Quantitative ultrasound of bone in male osteoporosis. *Osteoporos. Int.*, 2002, 13(5): 388–393
8. P. H. Nicholson, R. Alkalay. Quantitative ultrasound predicts bone mineral density and failure load in human lumbar vertebrae. *Clin. Biomech. (Bristol, Avon)*, 2007, 22(6): 623–629
9. F. Padilla, F. Jenson, V. Bousson, F. Peyrin, P. Laugier. Relationships of trabecular bone structure with quantitative ultrasound parameters: *In vitro* study on human proximal femur using transmission and backscatter measurements. *Bone*, 2008, 42(6): 1193–1202
10. K. A. Wear, S. Nagaraja, M. L. Dreher, S. L. Gibson. Relationships of quantitative ultrasound parameters with cancellous bone microstructure in human calcaneus *in vitro*. *J. Acoust. Soc. Am.*, 2012, 131(2): 1605–1612
11. D. Ta, W. Wang, K. Huang, Y. Wang, L. H. Le. Analysis of frequency dependence of ultrasonic backscatter coefficient in cancellous bone. *J. Acoust. Soc. Am.*, 2008, 124(6): 4083–4090
12. C. Chappard, P. Laugier, B. Fournier, C. Roux, G. Berger. Assessment of the relationship between broadband ultrasound attenuation and bone mineral density at the calcaneus using BUA imaging and DXA. *Osteoporos. Int.*, 1997, 7(4): 316–322
13. G. Haïat, et al. *In vitro* speed of sound measurement at intact human femur specimens. *Ultrasound Med. Biol.*, 2005, 31(7): 987–996
14. D. Hans, et al. Ultrasound velocity of trabecular cubes reflects mainly bone density and elasticity. *Calcif. Tissue Int.*, 1999, 64(1): 18–23
15. S. Mészáros, E. Tóth, V. Ferencz, E. Csupor, E. Hosszú, C. Horváth. Calcaneous quantitative ultrasound measurements predicts vertebral fractures in idiopathic male osteoporosis. *Joint Bone Spine*, 2007, 74(1): 79–84
16. W. Pluskiewicz, B. Drozdzowska. Ultrasonic measurement of the calcaneus in Polish normal and osteoporotic women and men. *Bone*, 1999, 24(6): 611–617
17. P. Laugier. An overview of bone sonometry. *Int. Congr. Ser.*, 2004, 1274: 23–32
18. K. A. Wear. Ultrasonic scattering from cancellous bone: A review. *IEEE Trans. Ultrason. Ferroelectr. Freq. Control*, 2008, 55(7): 1432–1441
19. B. K. Hoffmeister, A. P. Holt, S. C. Kaste. Effect of the cortex on ultrasonic backscatter measurements of cancellous bone. *Phys. Med. Biol.*, 2011, 56(19): 6243–6255
20. B. K. Hoffmeister, et al. Ultrasonic characterization of human cancellous bone in vitro using three different apparent backscatter parameters in the frequency range 0.6–15.0 MHz. *IEEE Trans. Ultrason. Ferroelectr. Freq. Control*, 2008, 55(7): 1442–1452
21. K. Il Lee, M. Joo Choi. Frequency-dependent attenuation and backscatter coefficients in bovine trabecular bone from 0.2 to 1.2 MHz. *J. Acoust. Soc. Am.*, 2012, 131(1): EL67–EL73
22. C. C. Liu, H. J. Han, D. A. Ta, W. Q. Wang. Effect of selected signals of interest on ultrasonic backscattering measurement in cancellous bones. *Sci. China Phys. Mech.*, 2013, 56(7): 1310–1316
23. C. C. Liu, D. Ta, B. Hu, L. H. Le, W. Wang. The analysis and compensation of cortical thickness effect on ultrasonic backscatter signals in cancellous bone. *J. Appl. Phys.*, 2014, 116(12): 124903
24. C. C. Liu, et al. The relationship between ultrasonic backscatter and trabecular anisotropic microstructure in cancellous bone. *J. Appl. Phys.*, 2014, 115(6): 064906
25. F. Padilla, F. Peyrin, P. Laugier. Prediction of backscatter coefficient in trabecular bones using a numerical model of three-dimensional microstructure. *J. Acoust. Soc. Am.*, 2003, 113(2): 1122–1129
26. K. A. Wear, A. Laib. The dependence of ultrasonic backscatter on trabecular thickness in human calcaneus: Theoretical and experimental results. *IEEE Trans. Ultrason. Ferroelectr. Freq. Control*, 2003, 50(8): 979–986
27. K. A. Wear, A. P. Stuber, J. C. Reynolds. Relationships of ultrasonic backscatter with ultrasonic attenuation, sound speed and bone mineral density in human calcaneus. *Ultrasound Med. Biol.*, 2000, 26(8): 1311–1316
28. B. S. Garra, M. Locher, S. Felker, K. A. Wear. Measurements of ultrasonic backscattered spectral centroid shift from spine *in vivo*: Methodology and preliminary results. *Ultrasound Med. Biol.*, 2009, 35(1): 165–168
29. K. Huang, D. Ta, W. Wang, L. H. Le. Simplified inverse filter tracking algorithm for estimating the mean trabecular bone spacing. *IEEE Trans. Ultra-*

son. Ferroelectr. Freq. Control, 2008, 55(7): 1453–1464

30. W. C. Pereira, S. L. Bridal, A. Coron, P. Laugier. Singular spectrum analysis applied to backscattered ultrasound signals from *in vitro* human cancellous bone specimens. *IEEE Trans. Ultrason. Ferroelectr. Freq. Control*, 2004, 51(3): 302–312
31. Y. Q. Jiang, et al. Analysis of apparent integrated backscatter coefficient and backscattered spectral centroid shift in Calcaneus *in vivo* for the ultrasonic evaluation of osteoporosis. *Ultrasound Med. Biol.*, 2014, 40(6): 1307–1317
32. R. Zhang, D. Ta, C. Liu, C. Chen. Feasibility of bone assessment with ultrasonic backscatter signals in neonates. *Ultrasound Med. Biol.*, 2013, 39(10): 1751–1759
33. J. Litniewski, L. Cieslik, M. Lewandowski, R. Tymkiewicz, B. Zienkiewicz, A. Nowicki. Ultrasonic scanner for *in vivo* measurement of cancellous bone properties from backscattered data. *IEEE Trans. Ultrason. Ferroelectr. Freq. Control*, 2012, 59(7): 1470–1477
34. J. P. Karjalainen, et al. Multi-site bone ultrasound measurements in elderly women with and without previous hip fractures. *Osteoporos. Int.*, 2012, 23(4): 1287–1295
35. C. Liu, et al. Signal of interest selection standard for ultrasonic backscatter in cancellous bone evaluation. *Ultrasound Med. Biol.*, 2015, 41(10): 2714–2721
36. M. S. Fewtrell, T. J. Cole, N. J. Bishop, A. Lucas. Neonatal factors predicting childhood height in preterm infants: Evidence for a persisting effect of early metabolic bone disease? *J. Pediatr.*, 2000, 137(5): 668–673
37. M. C. Backström, A. L. Kuusela, R. Mäki. Metabolic bone disease of prematurity. *Ann. Med.*, 1996, 28(4): 275–282
38. A. Lucas, O. G. Brooke, B. A. Baker, N. Bishop, R. Morley. High alkaline phosphatase activity and growth in preterm neonates. *Arch. Dis. Child.*, 1989, 64(7 Spec No): 902–909
39. J. E. Teitelbaum, et al. Quantitative ultrasound in the evaluation of bone status in premature and full-term infants. *J. Clin. Densitom.*, 2006, 9(3): 358–362
40. M. Catache, C. R. Leone. Role of plasma and urinary calcium and phosphorus measurements in early detection of phosphorus deficiency in very low birthweight infants. *Acta Paediatr.*, 2003, 92(1): 76–80
41. J. Faerk, B. Peitersen, S. Petersen, K. F. Michaelsen. Bone mineralisation in premature infants cannot be predicted from serum alkaline phosphatase or serum phosphate. *Arch. Dis. Child. Fetal Neonatal Ed.*, 2002, 87(2): F133–F136
42. W. W. K. Koo, J. Walters, A. J. Bush, R. W. Chesney, S. E. Carlson. Dual-energy X-ray absorptiometry studies of bone mineral status in newborn infants. *J. Bone Miner. Res.*, 1996, 11(7): 997–1002
43. H. McDevitt, S. F. Ahmed. Quantitative ultrasound assessment of bone health in the neonate. *Neonatology*, 2007, 91(1): 2–11
44. L. Pereda, T. Ashmeade, J. Zaritt, J. D. Carver. The use of quantitative ultrasound in assessing bone status in newborn preterm infants. *J. Perinatol.*, 2003, 23(8): 655–659
45. A. Omar, S. Turan, A. Bereket. Reference data for bone speed of sound measurement by quantitative ultrasound in healthy children. *Arch. Osteoporos.*, 2006, 1(1–2): 37–41
46. P. A. Narayana, J. Ophir. A closed form method for the measurement of attenuation in nonlinearly dispersive media. *Ultrason. Imaging*, 1983, 5(1): 17–21
47. B. Rack, et al. Ultrasound for the assessment of bone quality in preterm and term infants. *J. Perinatol.*, 2012, 32(3): 218–226